Thermodynamic Analysis of the Activation Mechanism of the GCSF Receptor Induced by Ligand Binding

Shouhei Mine,[‡,§] Takumi Koshiba,[∥] Eijiro Honjo,[‡] Tomoyuki Okamoto,[⊥] Taro Tamada,[‡,⊥] Yoshitake Maeda,[‡] Yasuko Matsukura,[‡] Akane Horie,[‡] Matsujiro Ishibashi,[@] Miharu Sato,[⊥] Mizue Azuma,[⊥] Masao Tokunaga,[@] Katsutoshi Nitta,[∥] and Ryota Kuroki*[,‡,⊥]

Pharmaceutical Research Laboratories, Kirin Brewery Company Ltd., 3 Miyahara-cho, Takasaki 370-1295, Japan, Central Laboratories for Key Technology, Kirin Brewery Company Ltd., 1-13-5 Fukuura, Kanazawa-ku, Yokohama 236-0004, Japan, Division of Biological Sciences, Graduate School of Science, Hokkaido University, Kita-ku, Sapporo 060-0810, Japan, Laboratory of Applied Microbiology, Faculty of Agriculture, Kagoshima University, 1-21-24 Korimoto, Kagoshima 890-0065, Japan, and Institute for Protein Research, Osaka University, 3-2 Yamadaoka, Suita, Osaka 565-0871, Japan

Received September 18, 2003; Revised Manuscript Received January 6, 2004

ABSTRACT: The granulocyte colony-stimulating factor receptor (GCSFR), containing the Ig-like domain (Ig) and cytokine receptor homologous region (CRH), was prepared as a preformed dimer (Ig-CRH-Fc)$_2$ after fusion to the mouse Fc region via an eight-residue linker (∼55 Å). Monomer Ig-CRH was also prepared after the Fc region was removed from (Ig-CRH-Fc)$_2$. GCSF binding to Ig-CRH and (Ig-CRH-Fc)$_2$ was investigated using light scattering and isothermal titration calorimetry. The average molecular mass determined by light scattering showed that both Ig-CRH and (Ig-CRH-Fc)$_2$ formed a 2:2 dimer with GCSF. Moreover, isothermal titration calorimetry showed that the thermodynamic parameters upon binding of GCSF to Ig-CRH and (Ig-CRH-Fc)$_2$ were comparable, suggesting a similar binding stoichiometry and interface [including similar buried surface area (5700−6000 Å^2)] despite the presence of the eight-residue linker. The buried surface area is much larger than that calculated from our previous report of the crystal structure of the GCSF−CRH complex [Aritomi, M., *et al*. (1999) *Nature 401*, 713−717], suggesting a substantial contribution of the Ig domain to GCSF binding. The data also indicate that the distance (55 Å) between two CRH domains in the 2:2 complex is much shorter than in our previous model (∼90 Å) predicted from the same crystal structure of the GCSF−CRH complex.

Granulocyte colony-stimulating factor (GCSF)[1] (*1*) is an important cytokine for regulating the maturation, proliferation, and differentiation of the precursor cells of neutrophic granulocytes and is used to treat patients suffering from granulopoenia. These responses are initiated by interaction of GCSF with the GCSF receptor (GCSFR) (*2*, *3*) which is expressed on neutrophils, their precursors, and some leukemic cell lines. Binding of GCSF causes receptor activation of signaling cascades such as the Jak-STAT and mitogen-activated protein kinase pathways (*4*).

The extracellular region of the GCSFR is composed of an immunoglobulin-like (Ig) domain, a cytokine receptor homologous (CRH) region, and three fibronectin type III-like domains (FNIII) (Figure 1a). The CRH region is divided into an amino-terminal (BN) domain and a carboxyl-terminal (BC) domain containing a "WSXWS" motif (*2*). These features of the GCSFR structure are closely related to that of gp130, which is the shared signal transducing receptor chain of the IL-6 family of cytokines (*5*). The sequences of the GCSFR and gp130 are 46% similar in the extracellular region (*6*).

The CRH region and Ig domain of the GCSFR have been implicated in ligand binding (*5*, *7*). Studies of sedimentation equilibrium experiments revealed that binding of GCSF to the extracellular region of the GCSFR results in the formation of a 2:2 complex (*8*, *9*). Recently, the crystal structure of GCSF in complex with the CRH region of the GCSFR has been determined, indicating that it forms a complex with 2:2 stoichiometry (*10*). However, Hiraoka *et al*. (*11*) reported that the BN and BC domains (the CRH region) formed a 1:1 complex with GCSF. In addition, the Ig domain of the GCSFR has been shown to be important for complex formation by chimeric receptor analysis (*12*) and mapping of neutralizing mAbs (*13*). Similarly, the crystal structure of gp130 in complex with viral IL-6 shows that the Ig domain of gp130 interacts with IL-6, resulting in formation of a tetramer comprised of two IL-6 and two gp130 subunits (*14*). These observations suggest that a complete understanding of the interaction requires a description of the biophysical properties that drive complex formation since the GCSF−Ig-CRH complex structure remains to be elucidated.

We have initiated an investigation of the quantitative and structural properties of the interaction of GCSF and its

* To whom correspondence should be addressed. Phone: +81-45-788-7240. Fax: +81-45-788-5186. E-mail: r-kuroki@kirin.co.jp.
‡ Pharmaceutical Research Laboratories, Kirin Brewery Co. Ltd.
§ Osaka University.
∥ Hokkaido University.
⊥ Central Laboratories for Key Technology, Kirin Brewery Co. Ltd.
@ Kagoshima University.

[1] Abbreviations: GCSF, granulocyte colony-stimulating factor; GCSFR, granulocyte colony-stimulating factor receptor; Ig, immunoglobulin; CRH, cytokine receptor homologous; IL, interleukin; ITC, isothermal titration calorimetry.

10.1021/bi0356855 CCC: $27.50
Published on Web 02/10/2004

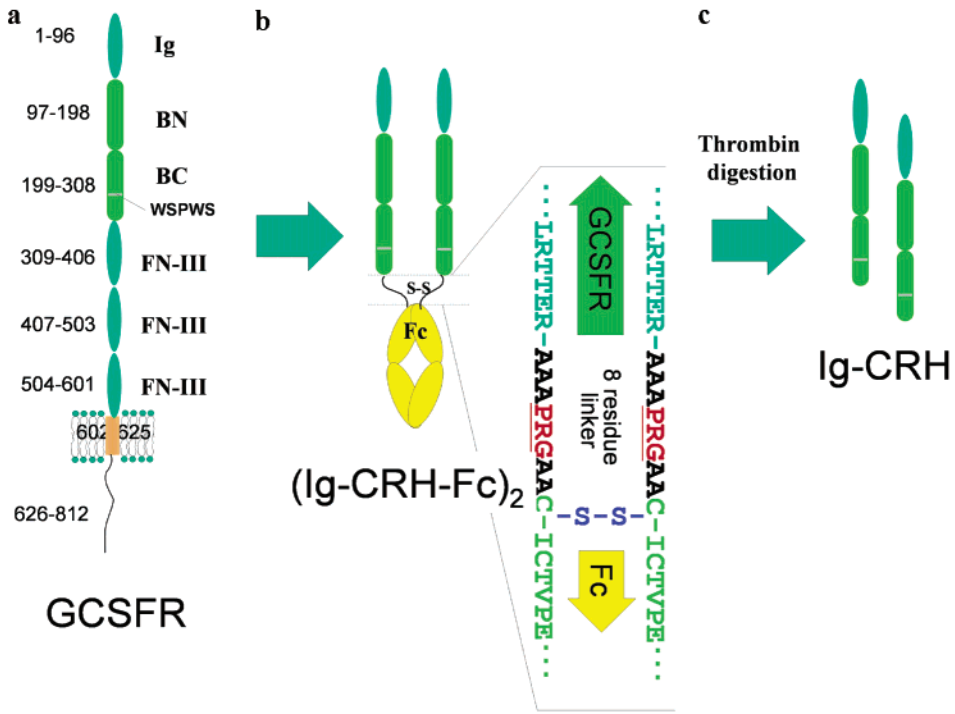

FIGURE 1: Diagrammatic representation of the subdomains of the wild-type GCSFR and the production of Ig-CRH via (Ig-CRH-Fc)$_2$. The BN and BC domains together comprise the CRH domain. The eight-residue linker sequence between Ig-CRH and Fc is also shown.

receptor. In this report, we describe the expression and production of baculovirus-expressed human Ig-CRH fused to an immunoglobulin Fc domain [(Ig-CRH-Fc)$_2$]. In addition to characterization of the interaction between GCSF and the Ig-CRH domains using size-exclusion chromatography and light scattering, we have investigated the thermodynamics of the interaction using isothermal titration calorimetry (ITC) to verify the binding stoichiometry and to more precisely determine dissociation constants for the complex. The ITC data also provide information about the enthalpy and the heat capacity change upon association, which reflects the conformational change as well as the buried surface area. The thermodynamic data for the GCSF−GCSFR interaction reported here suggest that the activated structure of the GCSFR induced by GCSF binding is a 2:2 complex structure, which is quite different from the reported crystal structure.

EXPERIMENTAL PROCEDURES

Materials. Recombinant human GCSF expressed in *Escherichia coli* was obtained from the Pharmaceutical Division of Kirin Brewery Co. Ltd. (Tokyo, Japan). Human thrombin was purchased from Roche Diagnostics GmbH (Mannheim, Germany).

Construction of Human GCSF Receptor cDNA Fused with the Fc Region of Mouse IgG1 (h-GCSFR-Fc) cDNA. The extracellular region of the human GCSF receptor (hGCSFR) containing an Ig-like domain (Ig) and cytokine receptor homologous region (CRH) [in which free cysteines at positions 78, 163, and 228 were mutated to serines (*15*)] was fused with the Fc region of mouse IgG1. To PCR amplify an Ig-CRH domain of hGCSFR cDNA, a forward primer (5′-TCTGAAGCTTGTTGCCCATATGGCAAGGCTGGGAAACTG-3′) was used. This primer also contained a *Bgl*II site upstream of the open reading frame and an *Nde*I site at a start codon 5′ of the hybridizing sequence. A reverse primer (5′-TGTAGAATTCGCGCCCGCCCGTTCGGTAGTTCTCAG-3′) was utilized and contained a *Not*I site. PCR was performed in a final volume of 100 μL for 25 cycles under the following temperature conditions: 94 °C for 15 s, 65 °C for 2 s, and 74 °C for 30 s. The PCR-amplified products were gel purified and digested with *Bgl*II and *Not*I restriction endonucleases. The cDNA of mouse IgG1 (TN1) derived from anti-human TPO IgG1 (*16*) was subcloned into a pBluescript II vector (Stratagene, La Jolla, CA). To amplify an Fc region of TN1 cDNA, a forward primer (5′-TCGTTCAAAGGCGGCCGCTCCCCGTGGCGCTGCCTGCAATCTGTACAGTCCCAGAAG-3′) was used. This primer also contained a *Not*I site at a start codon 5′ of the hybridizing sequence. The reverse primer (5′-GCTTAGCTCGAGTTATCATTTACCAGGAGAGTGGGA-3′) had an *Xho*I site downstream of the open reading frame. PCR in a final volume of 100 μL was carried out for 25 cycles under the following temperature conditions: 94 °C for 15 s, 65 °C for 2 s, and 74 °C for 30 s. The PCR-amplified products were gel purified and digested with *Not*I and *Xho*I restriction endonucleases. The baculovirus transfer vector, pFastBacl (Invitrogen, Carlsbad, CA), was digested with *Bam*HI and *Not*I restriction endonucleases. The individual PCR DNA fragments and the digested pFastBac1 vector DNA were ligated. Initial transformation and screening were carried out in *E. coli* DH5α, and the positive clones were confirmed by dideoxy sequencing and used for transformation of *E. coli* DH10Bac (Invitrogen).

Cell Culture and Virus. The Bac-To-Bac baculovirus (Invitrogen) is a derivative of *Autographa californica* nuclear polyhedrosis virus (AcMNPV). The recombinant virus was propagated in a monolayer culture of *Spodoptera frugiperda* (Sf9) cells. Serum-free medium-adapted Sf9 cells (Invitrogen) were grown in a monolayer culture at 27 °C in Grace's insect cell culture medium (Invitrogen) in the presence of a final

antibiotic−antimycotic (Invitrogen) concentration of 1×. *Trichoplusia ni*, High-Five cells (Invitrogen) adapted in serum-free medium were grown in a monolayer culture at 27 °C in High-Five serum-free medium according to the manufacturer's protocol (Invitrogen).

Generation of Recombinant Baculovirus. Generation of recombinant baculovirus-expressing hGCSFR-Fc in Sf9 cells was carried out by using the Bac-To-Bac baculovirus expression kit (Invitrogen). DNA of the recombinant pFastBac1 transfer vector containing the hGCSFR-Fc cDNA sequence was introduced into *E. coli* DH10Bac for the transposition of the hGCSFR-Fc cDNAs into baculovirus genomic DNA (bacmid) according to the manufacturer's protocol. Colonies containing recombinant bacmids were identified by disruption of the lacZα gene, and the white colonies were picked for recombinant bacmid DNA isolation. DNA was isolated using a Wizard SV Mini prep kit (Promega, Madison, WI) specific for DNA more than 135 kb long. The recombinant bacmid DNA was then used to transfect Sf9 cells which were grown in TNM-FH medium. The cells were transfected at a density of 1×10^6 cells/35 mm well with the bacmid DNA using Lipofectin according to the manufacturer's protocol (Invitrogen). The recombinant virus was harvested 72 h post-transfection and utilized for expression studies.

Expression and Purification of the Recombinant Protein. High-Five cells were grown in 75 mm tissue culture flasks till 70−80% confluency for use in the production of recombinant hGCSFR-Fc. The cells were infected with recombinant virus at different multiplicities of infection (MOI) at 27 °C for 72 h. The culture medium was collected 72 h postinfection followed by centrifugation at 10000*g* and 4 °C for 5 min and purified using the GCSF-coupled Sepharose column, which was prepared by mixing 2.0 mL of recombinant human GCSF per milliliter of NHS-activated Sepharose (Pharmacia). The bound protein was eluted with 50 mM glysine (pH 2.5) and immediately dialyzed to 20 mM HEPES and 100 mM NaCl (pH 7.2) at 4 °C.

Thrombin Digestion of (Ig-CRH-Fc)$_2$. Approximately 1 mg of (Ig-CRH-Fc)$_2$ was digested with 0.02 mg [1:50 (w/w)] of human thrombin (Roche Diagnostics GmbH) in 20 mM Tris-HCl buffer (pH 8.5) for 48 h at 37 °C.

Western Blot Analysis. For Western blot analysis, approximately 2 μg of cytoplasmic extract or 5 μL of culture medium supernatant was electrophoresed on a 7.5% polyacrylamide gel (Daiichi Pure Chemicals, Tokyo, Japan), and the resolved protein was transferred onto a nitrocellulose membrane (Millipore, Bedford, MA) according to the manufacturer's protocol. After being blocked with BSA, the membrane was probed with alkaline phosphatase-linked anti-mouse IgG (Biomeda Corp., Foster City, CA). hGCSFR-Fc was visualized with 5-bromo-4-chloro-3-indolylphosphate (BCIP) with nitro blue terazolium (NBT) (Promega, Madison, WI) according to the manufacturer's protocol.

Gel Filtration and Light Scattering Analysis. Gel filtration was performed using a Superdex 200 HR 10/30 column (Amersham Pharmacia Biotech AB, Uppsala, Sweden) equilibrated with 20 mM sodium phosphate buffer (pH 7.0) containing 200 mM NaCl. Light scattering analysis of the interaction between GCSF and Ig-CRH or (Ig-CRH-Fc)$_2$ was performed using mini-DAWN (Wyatt Technologies) equipped with a gel filtration column. Approximately 50 μg of GCSF and Ig-CRH or (Ig-CRH-Fc)$_2$ were injected onto a Superdex 200 column equilibrated with 20 mM sodium phosphate buffer (pH 7.0) containing 200 mM NaCl at a flow rate of 0.5 mL/min. The elution of the complex was monitored by both the refractive index and UV detectors.

Isothermal Titration Calorimetry. Thermodynamic analysis of the interaction between GCSF and Ig-CRH or (Ig-CRH-Fc)$_2$ was performed using an MCS isothermal titration calorimeter (MicroCal Inc., Northampton, MA). A 100 μM GCSF solution in 50 mM sodium phosphate buffer (pH 6.0) containing 100 mM NaCl was loaded into a 250 μL syringe, and 10 μL portions of the GCSF solution were injected into 1.6 mL of receptor solution (0.6 μM) in the same buffer. The titration curves were analyzed using ORIGIN (MicroCal Inc.).

The amount of apolar (ΔASA_{ap}) and polar (ΔSAS_{pol}) surface area buried upon binding were calculated from the empirical relationships to the binding heat capacity (ΔC_p) and enthalpy (ΔH) changes as

$$\Delta C_p = 0.45 \times \Delta ASA_{ap} - 0.26 \times \Delta SAS_{pol} \quad (1)$$

$$\Delta H_{60} = -8.44 \times \Delta ASA_{ap} + 31.4 \times \Delta SAS_{pol} \quad (2)$$

where ΔH_{60} is the binding enthalpy change at 60 °C (*17*, *18*).

RESULTS

Expression and Purification of Ig-CRH Fused with Fc. For effective expression, the Ig-CRH was fused to the Fc domain derived from mouse IgG to create a disulfide cross-linked dimer of the receptors [(Ig-CRH-Fc)$_2$]. The linker region with the disulfide bridge was designed to limit the receptor distance to <55 Å, and a thrombin cut site was incorporated so that the Ig-CRH domain can be cleaved if necessary (Figure 1a). The designed sequence is shown in Figure 1b.

The purified (Ig-CRH-Fc)$_2$ exhibited a single band with a molecular mass of 140 kDa under nonreducing conditions and of 70 kDa under reducing conditions on SDS−PAGE (see Figure 2), indicating the protein is present as a disulfide-linked dimer. The molecular mass of 140 kDa for (Ig-CRH-Fc)$_2$ is somewhat higher than that calculated from the amino acid sequence (125 kDa), suggesting glycosylation at four potential N-linked glycosylation sites within the Ig-CRH region (*19*). When tunicamycin, a glycosylation inhibitor, was added to the culture medium after infection, the molecular mass of (Ig-CRH-Fc)$_2$ was reduced to 125 kDa, supporting the proposed glycosylation within the Ig-CRH region (data not shown).

(Ig-CRH-Fc)$_2$ was digested by thrombin to prepare the monomer Ig-CRH. The time course of thrombin digestion is shown in Figure 3. After digestion for 48 h, (Ig-CRH-Fc)$_2$ was completely digested to monomer Ig-CRH and the Fc domain. The digested Ig-CRH was purified by gel filtration and used for all characterization studies as described below.

Gel Filtration and Light Scattering Analysis of the GCSF−Ig-CRH Complex. Gel filtration and light scattering analysis of each protein, alone and as a ligand−receptor complex, were utilized to further probe the receptor−ligand interactions and binding stoichiometry (Figure 4 and Table 1). The size-

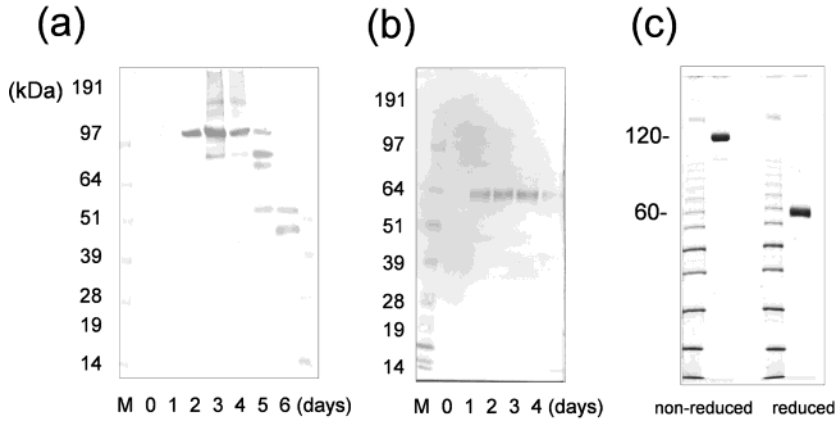

FIGURE 2: Expression and purification of $(Ig\text{-}CRH\text{-}Fc)_2$ monitored by SDS−PAGE. (a) Time course of the expression analyzed under nonreducing conditions: lane M, molecular mass markers; and lanes 0−6, elapsed time in days postinfection. (b) Time course of the expression analyzed under reducing conditions as with panel a. (c) Purified $(Ig\text{-}CRH\text{-}Fc)_2$ analyzed under reducing and nonreducing conditions.

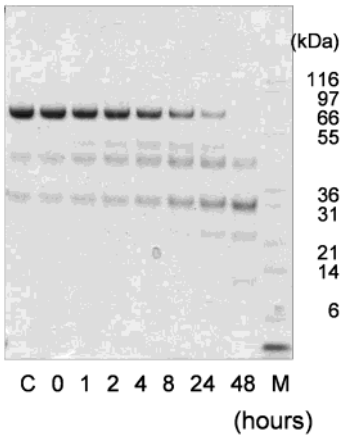

FIGURE 3: Thrombin digestion of $(Ig\text{-}CRH\text{-}Fc)_2$ to remove the Fc portion. Thrombin cleavage was monitored by SDS−PAGE under reducing conditions: lane C, control experiment without thrombin; lane M, molecular mass markers; and lanes 0, 1, 2, 4, 8, 24, and 48, elapsed time in hours after thrombin digestion.

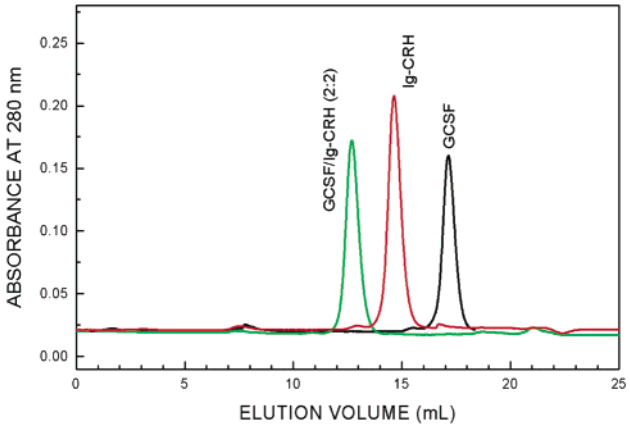

FIGURE 4: Gel filtration of GCSF, Ig-CRH, and the GCSF−Ig-CRH complex using a Superdex 200 column at pH 7.0. The GCSF−Ig-CRH complex was prepared by mixing equal molar amounts of GCSF and Ig-CRH.

exclusion chromatograms of GCSF and Ig-CRH as well as the average molecular masses of these proteins indicate that each protein exists as a monomer. Moreover, gel filtration of a stoichiometric mixture between GCSF and Ig-CRH showed a single peak (Figure 4). The average molecular mass of this peak was determined to be 111 600 ± 2460 Da by light scattering analysis. Since the theoretical molecular masses of GCSF and Ig-CRH are 18 670 and 34 320 Da, respectively, the observed mass of this peak indicates that GCSF and Ig-CRH formed a 2:2 stoichiometric complex under this condition.

Table 1: Average Molecular Mass of GCSF and Its Receptor Complex Determined by Light Scattering Analysis

receptor	observed mass (Da)	theoretical mass (Da)
GSCF	17910 ± 890	19000
Ig-CRH	36950 ± 860	36000
GCSF−Ig-CRH	111600 ± 2460	56000 (1:1) 112000 (2:2)

Hiraoka and co-workers also expressed murine Ig-CRH in baculovirus cells and characterized the human GCSF−murine Ig-CRH interactions using sedimentation equilibrium centrifugation (*20*). This group observed the self-association of the murine Ig-CRH dimer converted to an octameric complex containing four receptors and four GCSF molecules, which was not detected in our studies. It is possible that this difference may be partly due to the different species, human and murine receptor, and to the number of N-linked glycosylation sites.

Isothermal Titration Calorimetry of GCSF Binding to Ig-CRH and (Ig-CRH-Fc)₂. To understand the nature of the active state of the GCSFR, the thermodynamic parameters of the binding of GCSF to Ig-CRH and $(Ig\text{-}CRH\text{-}Fc)_2$ were investigated using isothermal titration calorimetry (ITC). The results are summarized in Table 2. The titration of Ig-CRH with GCSF showed negative peaks (Figure 5b), indicating an exothermic process upon binding to Ig-CRH. The thermodynamic parameters of binding of GCSF to Ig-CRH were as follows: $K_a = 7.2 \times 10^8\ M^{-1}$, $\Delta H = -99.5$ kJ/mol, and $n = 1$ at 25 °C, indicating an equimolar interaction such as a 1:1 or 2:2 complex. Moreover, the binding of GCSF to the preformed dimer, $(Ig\text{-}CRH\text{-}Fc)_2$, was also investigated to clarify the effect of preassociation of a receptor dimer. The titration also showed a single phase (Figure 5a) with the following thermodynamic parameters: $K_a = 2.6 \times 10^8\ M^{-1}$, $\Delta H = -95.6$ kJ/mol, and $n = 1.7$ at 26 °C, suggesting a 1:2 complex. The ITC results demonstrated that binding of GCSF to Ig-CRH and $(Ig\text{-}CRH\text{-}Fc)_2$ is an enthalpy-driven process (Table 2). Formation of hydrophobic and electrostatic contacts and hydrogen bonds between the ligand and receptor could account for the largely exothermic reaction ($\Delta H < 0$)

Table 2: Thermodynamic Parameters of the Binding of GCSF to Ig-CRH and (Ig-CRH-Fc)$_2$ Measured at Different Temperatures

receptor	temp (°C)	n	K_a ($\times 10^8$ M^{-1})	ΔH (kJ/mol)	ΔS^a (J mol^{-1} K^{-1})
Ig-CRH	15	1.0	2.4 ± 0.8	−66.6 ± 0.7	−70.0
	20	1.0	6.2 ± 1.7	−83.7 ± 0.5	−116.2
	25	1.0	7.2 ± 1.6	−99.5 ± 0.5	−164.0
	30	1.0	5.1 ± 1.7	−119.0 ± 1.0	−225.5
	35	1.1	6.8 ± 1.4	−131.0 ± 0.7	−255.4
(Ig-CRH-Fc)$_2$	17	1.7	2.9 ± 1.3	−66.0 ± 0.7	−64.8
	20	1.8	7.6 ± 1.5	−72.0 ± 0.5	−75.4
	26	1.7	2.6 ± 0.7	−95.6 ± 0.4	−159.0
	30	1.8	6.4 ± 0.7	−110.0 ± 0.4	−193.0
	35	1.6	3.3 ± 4.7	−134.0 ± 3.1	−271.6

[a] The ΔS values were calculated using the equations $\Delta G = -RT \ln K$ and $\Delta G = \Delta H - T\Delta S$. All thermodynamic parameters are expressed as per one binding site.

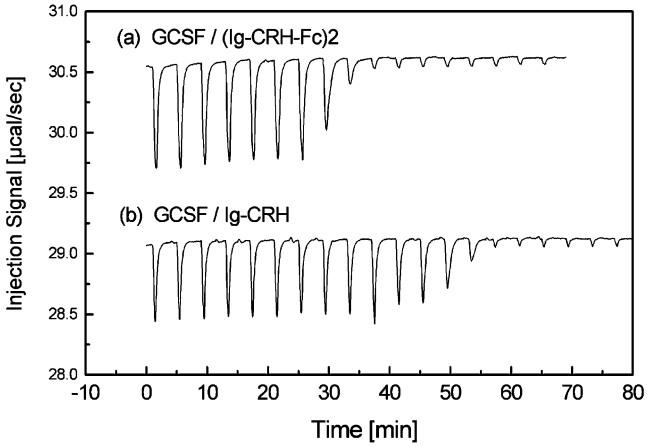

FIGURE 5: Titration calorimetry signals of (a) Ig-CRH and (b) (Ig-CRH-Fc)$_2$ by GCSF at pH 6.0 and 25 °C.

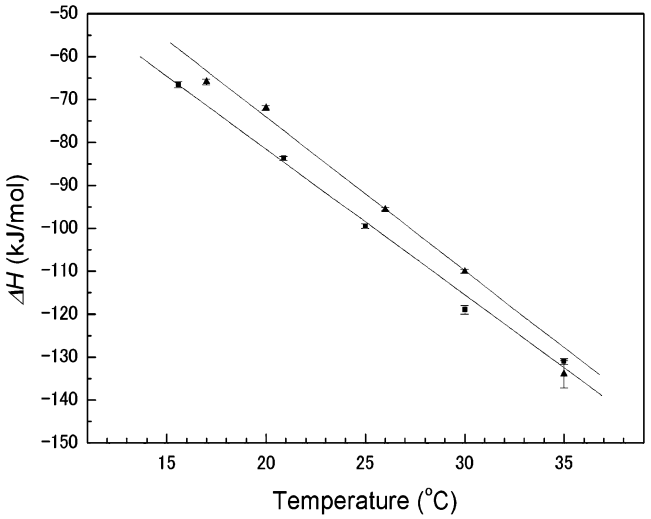

FIGURE 6: Temperature dependence plot of ΔH. ΔH values for the binding of GCSF to Ig-CRH (■) and (Ig-CRH-Fc)$_2$ (▲) are shown.

observed in the ITC measurements. The change in hydrophobic surface area of a protein upon binding to its ligand can be estimated by the change in heat capacity (ΔC_p), which can be determined from the enthalpy of binding (ΔH) measured at different temperatures (Figure 6). The ΔC_p values of binding of GCSF to Ig-CRH and (Ig-CRH-Fc)$_2$ were determined to be approximately -3.4 ± 0.05 and -3.6 ± 0.05 kJ mol^{-1} K^{-1}, respectively. Both ΔC_p values are similar, suggesting that the change in hydrophobic area upon GCSF binding could be similar for Ig-CRH and (Ig-CRH-Fc)$_2$. By using empirical relationships developed by Freire and colleagues (see Experimental Procedures), the ΔC_p and ΔH values observed for one molecule of GCSF binding to Ig-CRH and (Ig-CRH-Fc)$_2$ infer that 5700−6000 Å^2 of surface area is buried during complex formation. The thermodynamics of the binding of GCSF to Ig-CRH and (Ig-CRH-Fc)$_2$ are almost comparable within experimental error, despite the preassociation of Ig-CRH, suggesting an equivalent GCSF recognition mechanism.

DISCUSSION

We have expressed the soluble fragment of the GCSFR [(Ig-CRH-Fc)$_2$] in a baculovirus system for the purpose of studying the thermodynamic interaction of the GCSFR with GCSF in solution. The results of the light scattering and ITC analyses showed that GCSF has strong affinity ($K_a \sim 10^8$ M^{-1}) for Ig-CRH and the GCSF:Ig-CRH stoichiometry is 2:2. The affinity is almost identical to that of the full-length receptor expressed on the cell surface (*5*). Since there are almost no available data regarding direct thermodynamic parameters for GCSF−GCSFR interactions, our results provide new insights into GCSF−GCSFR interactions.

Thermodynamic analysis revealed that there were no remarkable differences in the thermodynamic parameters upon the binding of GCSF to Ig-CRH and (Ig-CRH-Fc)$_2$ even at different temperatures (Table 2 and Figure 6). Binding of GCSF to Ig-CRH or (Ig-CRH-Fc)$_2$ exhibited highly favorable binding enthalpy ($\Delta H < 0$), suggesting a large number of nonbonded interactions (e.g., hydrophobic and electrostatic interactions and hydrogen bonds) upon complex formation. Conversely, the binding entropy change for each reaction was extremely unfavorable, indicating a substantial loss of degrees of freedom upon binding. The thermodynamic changes upon binding of GCSF to Ig-CRH or (Ig-CRH-Fc)$_2$ suggest that these interactions accompany substantial conformational rearrangements such as local folding during GCSF binding.

Another common feature seen in the binding of GCSF to Ig-CRH and (Ig-CRH-Fc)$_2$ was a similar temperature dependence of their binding enthalpies (Figure 6), and ΔC_p values of −3.4 and −3.6 kJ mol^{-1} K^{-1} for Ig-CRH and (Ig-CRH-Fc)$_2$, respectively. Generally, large negative heat capacities have been found to correspond to the exclusion of highly ordered water molecules from exposed hydrophobic areas on unfolded proteins or free ligands (*21*−*23*). Since the ΔC_p values for protein−protein interactions have been reported to range from 0.01 to −1.34 kJ mol^{-1} K^{-1} (*24*), the ΔC_p values for GCSF are significantly larger than that typically observed for protein−protein interactions, suggesting that extensive apolar surface area is buried upon complex formation.

According to the consideration of Murphy *et al.* (*25*), the total ΔS of binding is given as

$$\Delta S = \Delta S_{solv} + \Delta S_{conf} + \Delta S_{crat} \quad (3)$$

where ΔS_{solv} is the change in entropy resulting from solvent release upon binding, ΔS_{conf} is the change in entropy resulting from configurational changes in the complex formation, and ΔS_{crat} is the cratic entropy change.

Table 3: Entropy Change (J mol^{-1} K^{-1}) in the Binding of GSCF to Ig-CRH and $(Ig\text{-}CRH\text{-}Fc)_2$ Measured at 25 °C

receptor	total ΔS	$\Delta\Delta S$	ΔS_{solv}	$\Delta\Delta S_{solv}$	ΔS_{conf}	$\Delta\Delta S_{conf}$
Ig-CRH	−164	0	870	0	−1037	0
$(Ig\text{-}CRH\text{-}Fc)_2$	−159	5	920	50	−1082	−45

ΔS_{solv} is given by

$$\Delta S_{solv} = \Delta C_p \ln(T/T_s) \quad (4)$$

where T_s is the temperature at which the dissolution entropy change is considered to be zero and ΔS_{crat} can be considered a constant value (−0.033 kJ mol^{-1} K^{-1}) (*26*). From eqs 3 and 4, the calculated values of entropy change are summarized in Table 3. In the binding of GCSF to $(Ig\text{-}CRH\text{-}Fc)_2$, ΔS_{solv} is ∼50 J mol^{-1} K^{-1} larger than that for the binding to Ig-CRH, indicating a smaller effect of water release upon binding of GCSF to $(Ig\text{-}CRH\text{-}Fc)_2$. This suggests some interaction between the two Ig-CRH domains cross-linked to Fc. Conversely, ΔS_{conf} for binding of GCSF to $(Ig\text{-}CRH\text{-}Fc)_2$ is ∼50 J mol^{-1} K^{-1} smaller than that for the binding to Ig-CRH, suggesting a restriction of the flexibility due to the cross-linking. The contribution of cross-linking to the total entropy change (ΔS) for binding of GCSF to $(Ig\text{-}CRH\text{-}Fc)_2$ appears to be relatively small, most likely due to the compensation between the decrease in the conformational entropy change (ΔS_{conf}) and the increase in the desolvation entropy change (ΔS_{solv}). In brief, the similar thermodynamics of binding of GCSF to Ig-CRH and $(Ig\text{-}CRH\text{-}Fc)_2$ indicate that they bind with a similar overall mechanism. The Fc portion serves as the fobronectin-like domains, which are not required for ligand binding but may be important for receptor stability and signal transduction (*5*).

From our experiments, it is now clear that binding of GCSF to Ig-CRH results in the formation of a 2:2 complex. Although there is no tertiary structural evidence, it has been hypothesized (*27*) that one GCSF molecule interacts with two receptors at independent sites, one receptor via site II and another receptor via site III. Site II is the main receptor binding site and lies within the A and C helices of GCSF involving charged residues (*10*, *12*, *28*, *29*). This site interacts with the "elbow" formed by the BN and BC domains of the CRH region (*10*). On the other hand, it has been suggested that the second receptor binding site (site III) is located near the N-terminal end of the D helix (*28*) or in the E helix of GCSF (*12*), forming a hydrophobic cluster. Site III is likely to be important for interaction with the Ig domain (*12*, *15*), and the recent analyses from the mutagenesis of the Ig domain have shown that the predicted F and G β-strands form a binding site for site III of GCSF (*27*). From the thermodynamic data, approximately 5700−6000 $Å^2$ of surface area is buried when one molecule of GCSF binds Ig-CRH. This value is much greater than the value of 1284 $Å^2$ observed in the crystallographic structure of the GCSF−CRH complex interface (*10*), suggesting that both complex structures are different with or without the Ig domain. Burial of a large surface area upon the interaction of GCSF and Ig-CRH also indicates the existence of an interaction between site III of GCSF and the Ig domain, and suggests that dramatic structural changes occur upon complex formation, e.g., local folding-coupled interactions. There is no doubt as to the importance of the contribution of the Ig domain upon formation of the active ligand−receptor complex in the GCSFR.

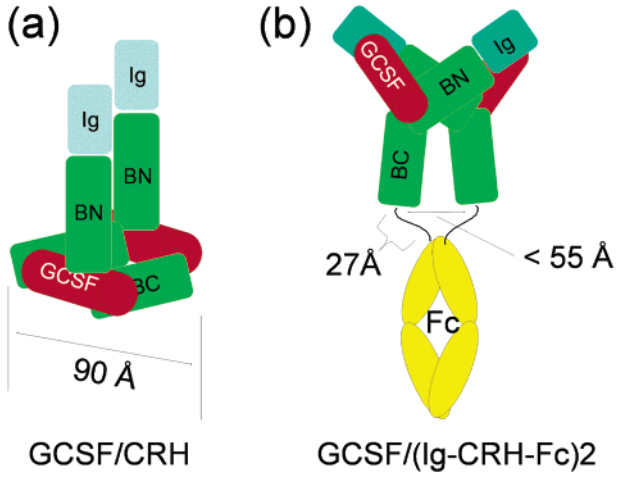

FIGURE 7: Receptor orientation of the active state of GCSFR. (a) Crystal structure of the GCSF−CRH complex (without the Ig domain) (*10*). (b) Receptor orientation satisfying the experimental data supplied in this report.

It has also been hypothesized that the activating efficiency of the cytokine receptor depends critically on the separation, orientation, and relative disposition of bound receptors (*30*−*34*). The thermodynamic analysis of the cross-linked dimer of Ig-CRH [$(Ig\text{-}CRH\text{-}Fc)_2$] connected by a flexible linker peptide between the Ig-CRH domain and the Fc portion allowed us to probe the distance between the insertion points of the extracellular domain dimer. At least two structural models have been proposed for the activated state of the GCSFR. One model, from the structural determination of the GCSF−CRH complex (*10*) in which two CRHs are bridged by two GCSFs, but with no information regarding the contribution of the Ig domain, is shown in Figure 7a. Another model, predicted from the structure of the IL-6−gp130 complex (*14*) in which both Ig and CRH domains are clearly involved in the binding with GSCF, is shown in Figure 7b. The distance between the carboxy terminus of the CRH domains (∼90 Å) in the crystal structure of the GCSF−CRH complex (Figure 7a) does not agree with the distance (<55 Å) between the carboxy termini in $(Ig\text{-}CRH\text{-}Fc)_2$ estimated from the length of the eight-amino acid linker (∼3.3 Å per residue) (Figure 7b). Thus, the model that is in agreement with the large buried surface area, as well as the shorter distance between the two CRHs (55 Å), is the one resembling the IL-6−gp130 complex (*14*) as shown in Figure 7b. The Ig domain would bring each CRH domain closer and facilitate the interaction of their intracellular domains. Therefore, without the Ig domain, the previously described 2:2 complex structure may involve a crystallographic artifact in which two 1:1 complexes are occasionally associated under the crystallization condition.

REFERENCES

1. Nagata, S., Tsuchiya, M., Asano, S., Kaziro, Y., Yamazaki, T., Yamamoto, O., Hirata, Y., Kubota, N., Oheda, M., Nomura, H., and Ono, M. (1986) Molecular cloning and expression of cDNA for human granulocyte colony-stimulating factor, *Nature 319*, 415−418.
2. Fukunaga, R., Ishizaka-Ikeda, E., Seto, Y., and Nagata, S. (1990) Expression cloning of a receptor for murine granulocyte colony-stimulating factor, *Cell 61*, 341−350.

3. Fukunaga, R., Seto, Y., Mizushima, S., and Nagata, S. (1990) Three different mRNAs encoding human granulocyte colony-stimulating factor receptor, *Proc. Natl. Acad. Sci. U.S.A. 87*, 8702−8706.
4. Avalos, B. R. (1996) Molecular analysis of the granulocyte colony-stimulating factor receptor, *Blood 88*, 761−777.
5. Fukunaga, R., Ishizaka-Ikeda, E., Pan, C. X., Seto, Y., and Nagata, S. (1991) Functional domains of the granulocyte colony-stimulating factor receptor, *EMBO J. 10*, 2855−2865.
6. Hammacher, A., Richardson, R. T., Layton, J. E., Smith, D. K., Angus, L. J., Hilton, D. J., Nicola, N. A., Wijdenes, J., and Simpson, R. J. (1998) The immunoglobulin-like module of gp130 is required for signaling by interleukin-6, but not by leukemia inhibitory factor, *J. Biol. Chem. 273*, 22701−22707.
7. Layton, J. E., Iaria, J., Smith, D. K., and Treutlein, H. R. (1997) Identification of a ligand-binding site on the granulocyte colony-stimulating factor receptor by molecular modeling and mutagenesis, *J. Biol. Chem. 272*, 29735−29741.
8. Horan, T., Wen, J., Narhi, L., Parker, V., Garcia, A., Arakawa, T., and Philo, J. (1996) Dimerization of the extracellular domain of granuloycte-colony stimulating factor receptor by ligand binding: a monovalent ligand induces 2:2 complexes, *Biochemistry 35*, 4886−4896.
9. Horan, T. P., Martin, F., Simonet, L., Arakawa, T., and Philo, J. S. (1997) Dimerization of granulocyte-colony stimulating factor receptor: the Ig plus CRH construct of granulocyte-colony stimulating factor receptor forms a 2:2 complex with a ligand, *J. Biochem. 121*, 370−375.
10. Aritomi, M., Kunishima, N., Okamoto, T., Kuroki, R., Ota, Y., and Morikawa, K. (1999) Atomic structure of the GCSF-receptor complex showing a new cytokine-receptor recognition scheme, *Nature 401*, 713−717.
11. Hiraoka, O., Anaguchi, H., Asakura, A., and Ota, Y. (1995) Requirement for the immunoglobulin-like domain of granulocyte colony-stimulating factor receptor in formation of a 2:1 receptor−ligand complex, *J. Biol. Chem. 270*, 25928−25934.
12. Layton, J. E., Shimamoto, G., Osslund, T., Hammacher, A., Smith, D. K., Treutlein, H. R., and Boone, T. (1999) Interaction of granulocyte colony-stimulating factor (G-CSF) with its receptor. Evidence that Glu19 of G-CSF interacts with Arg288 of the receptor, *J. Biol. Chem. 274*, 17445−17451.
13. Layton, J. E., Iaria, J., and Nicholson, S. E. (1997) Neutralising antibodies to the granulocyte colony-stimulating factor receptor recognise both the immunoglobulin-like domain and the cytokine receptor homologous domain, *Growth Factors 14*, 117−130.
14. Chow, D., He, X., Snow, A. L., Rose-John, S., and Garcia, K. C. (2001) Structure of an extracellular gp130 cytokine receptor signaling complex, *Science 291*, 2150−2155.
15. Ishibashi, M., Tokunaga, H., Arakawa, T., and Tokunaga, M. (2001) Expression, purification, and characterization of the active immunoglobulin-like domain of human granulocyte-colony-stimulating factor receptor in *Escherichia coli*, *Protein Expression Purif. 21*, 317−322.
16. Tahara, T., Kuwaki, T., Matsumoto, A., Morita, H., Watarai, H., Inagaki, Y., Ohashi, H., Ogami, K., Miyazaki, H., and Kato, T. (1998) Native thrombopoietin: structure and function, *Stem Cells 16*, 54−60.
17. Xie, D., and Freire, E. (1994) Molecular basis of cooperativity in protein folding. V. Thermodynamic and structural conditions for the stabilization of compact denatured states, *Proteins 19*, 291−301.
18. Murphy, K. P., and Freire, E. (1992) Thermodynamics of structural stability and cooperative folding behavior in proteins, *Adv. Protein Chem. 43*, 313−361.
19. Haniu, M., Horan, T., Arakawa, T., Le, J., Katta, V., Hara, S., and Rohde, M. F. (1996) Disulfide structure and *N*-glycosylation sites of an extracellular domain of granulocyte-colony stimulating factor receptor, *Biochemistry 35*, 13040−13046.
20. Hiraoka, O., Anaguchi, H., and Ota, Y. (1994) Evidence for the ligand-induced conversion from a dimer to a tetramer of the granulocyte colony-stimulating factor receptor, *FEBS Lett. 356*, 255−260.
21. Spolar, R. S., and Record, M. T., Jr. (1994) Coupling of local folding to site-specific binding of proteins to DNA, *Science 263*, 777−784.
22. Livingstone, J. R., Spolar, R. S., and Record, M. T., Jr. (1991) Contribution to the thermodynamics of protein folding from the reduction in water-accessible nonpolar surface area, *Biochemistry 30*, 4237−4244.
23. Jelesarov, I., and Bosshard, H. R. (1994) Thermodynamics of ferredoxin binding to ferredoxin:$NADP^+$ reductase and the role of water at the complex interface, *Biochemistry 33*, 13321−13328.
24. Stites, W. E. (1997) Protein−Protein Interactions: Interface Structure, Binding Thermodynamics, and Mutational Analysis, *Chem. Rev. 97*, 1233−1250.
25. Murphy, K. P., Freire, E., and Peterson, Y. (1995) Configurational effects in antibody−antigen interactions studied by microcalorimetry, *Proteins 21*, 83−90.
26. Murphy, K. P., Privalov, P. L., and Gill, S. J. (1990) Common features of protein unfolding and dissolution of hydrophobic compounds, *Science 247*, 559−561.
27. Layton, J. E., Hall, N. E., Connell, F., Venhorst, J., and Treutlein, H. R. (2001) Identification of ligand-binding site III on the immunoglobulin-like domain of the granulocyte colony-stimulating factor receptor, *J. Biol. Chem. 276*, 36779−36787.
28. Reidhaar-Olson, J. F., De Souza-Hart, J. A., and Selick, H. E. (1996) Identification of residues critical to the activity of human granulocyte colony-stimulating factor, *Biochemistry 35*, 9034−9041.
29. Young, D. C., Zhan, H., Cheng, Q. L., Hou, J., and Matthews, D. J. (1997) Characterization of the receptor binding determinants of granulocyte colony stimulating factor, *Protein Sci. 6*, 1228−1236.
30. Livnah, O., Stura, E. A., Johnson, D. L., Middleton, S. A., Mulcahy, L. S., Wrighton, N. C., Dower, W. J., Jolliffe, L. K., and Wilson, I. A. (1996) Functional mimicry of a protein hormone by a peptide agonist: the EPO receptor complex at 2.8 Å, *Science 273*, 464−471.
31. Syed, R. S., Reid, S. W., Li, C., Cheetham, J. C., Aoki, K. H., Liu, B., Zhan, H., Osslund, T. D., Chirino, A. J., Zhang, J., Finer-Moore, J., Elliott, S., Sitney, K., Katz, B. A., Matthews, D. J., Wendoloski, J. J., Egrie, J., and Stroud, R. M. (1998) Efficiency of signalling through cytokine receptors depends critically on receptor orientation, *Nature 395*, 511−516.
32. Livnah, O., Johnson, D. L., Stura, E. A., Farrell, F. X., Barbone, F. P., You, Y., Liu, K. D., Goldsmith, M. A., He, W., Krause, C. D., Pestka, S., Jolliffe, L. K., and Wilson, I. A. (1998) An antagonist peptide-EPO receptor complex suggests that receptor dimerization is not sufficient for activation, *Nat. Struct. Biol. 5*, 993−1004.
33. Livnah, O., Stura, E. A., Middleton, S. A., Johnson, D. L., Jolliffe, L. K., and Wilson, I. A. (1999) Crystallographic evidence for preformed dimers of erythropoietin receptor before ligand activation, *Science 283*, 987−990.
34. Remy, I., Wilson, I. A., and Michnick, S. W. (1999) Erythropoietin receptor activation by a ligand-induced conformation change, *Science 283*, 990−993.

BI0356855